Journal of Magnetic Resonance **143,** 144–152 (2000)
doi:10.1006/jmre.1999.1986, available online at http://www.idealibrary.com on IDEAL®

Dielectric Resonator-Based Side-Access Probe for Muscle Fiber EPR Study

Andrzej Sienkiewicz,*,† Marek Jaworski,* Brian G. Smith,† Piotr G. Fajer,‡ and Charles P. Scholes§,[1]

*Institute of Physics, Polish Academy of Sciences, Al. Lotnikow 32/46, 02-668 Warsaw, Poland; †Department of Physics and §Department of Chemistry, State University of New York at Albany, 1400 Washington Avenue, Albany, New York 12222; and ‡National High Magnetic Field Laboratory, 1800 E. Paul Dirac Drive, Tallahassee, Florida 32306

Received July 13, 1999; revised November 15, 1999

We present a novel dielectric resonator (DR)-based resonant structure that accommodates aqueous sample capillaries in orientations that are either parallel (i.e., side-access) or perpendicular to the direction of an external (Zeeman) magnetic field, B_0. The resonant structure consists of two commercially available X-band DRs that are separated by a Rexolite spacer and resonate in the fundamental $TE_{01\delta}$ mode. The separator between the DRs is used to tune the resonator to the desired frequency and, by appropriately drilled sample holes, to provide access for longitudinal samples, notably capillaries containing oriented, spin-labeled muscle fibers. In contrast to the topologically similar cylindrical TE_{011} cavity, the DR-based structure has distinct microwave properties that favor its use for parallel orientation of lossy aqueous samples. For perpendicular orientation of a dilute (6.25 μM) aqueous solution of IASL spin label, the *S*/*N* ratio was at least one order of magnitude better for the side-access DR-based structure than for a standard TE_{102} cavity. EPR spectra acquired for maleimide spin-labeled myosin filaments also revealed ca. 10 times better *S*/*N* ratio than those obtained with a standard TE_{102} cavity. For the side-access DR with sample capillaries oriented either parallel or perpendicular to the external magnetic field, the *Q*- and filling factors are in good agreement with the theoretical estimates derived from the distribution of magnetic (H_1) and electric (E_1) components.

Key Words: **dielectric resonator; side-access; EPR resonator.**

1. INTRODUCTION

Actomyosin, a complex of actin filaments and myosin motor proteins, is responsible for force generation during muscle contraction. After 30 years of effort involving many biophysical techniques, models of the individual mechanical events at the molecular level of actomyosin, known as Huxley's "tilting cross-bridge" model (*1*, *2*), and its recent refinement, "lever-arm" hypothesis (*3*), still require experimental verification. It is commonly accepted that during muscle contraction, the changes in orientation of myosin heads that form cross-bridges between thick (myosin) and thin (actin) filaments are associated with the process of force generation. The central goal in muscle biophysics has been to detect such force-generating structural changes in the actomyosin cross-bridge complex. Since muscle proteins reveal a high degree of cylindrical ordering, orientation-sensitive spin probes attached to myosin heads in combination with electron paramagnetic resonance (EPR) spectroscopy have proven to be a powerful tool for detection of conformational changes within the myosin heads and, therefore, for testing of the cross-bridge model (*4*). The EPR spectrum of nitroxide spin labels attached to specific sites of the myosin heads is primarily sensitive to the orientation of their three principal axes, *x*, *y*, and *z*, relative to the external magnetic field, H_0 (*5*, *6*). On the other hand, the myosin heads are highly oriented relative to the muscle fiber axis, especially at the end of the power stroke. Thus, to follow the molecular reorientation of myosin heads relative to actin, there is a rationale for measuring EPR spectra of spin-labeled muscle fibers inserted into longitudinal capillaries and oriented either parallel or perpendicular with respect to H_0 (*7*, *8*). The EPR features acquired for these two orientations of the sample capillary reveal the highest degree of spectral differentiation (*9*). From the experimental standpoint, for either orientation of the sample capillary the microwave magnetic component, H_1, has to be applied perpendicular to H_0 in order to get the maximum probability of allowed resonant transitions, $\Delta M_s = \pm 1$, for the $S = \frac{1}{2}$ spin system of the nitroxide spin label (*10*). This precludes a simple cavity rotation by 90° (in the vertical plane) for changing the orientation of the spin-labeled muscle fiber from perpendicular to parallel. Equally, inserting the spin-labeled muscle fiber horizontally into a typical microwave cavity through an orifice in its front wall would result in a standard, perpendicular orientation (the fiber axis would still be perpendicular to H_0). Thus, the prerequisite feature of resonant structures for the EPR study of muscle fibers is their possibility of accommodating longitudinal, lossy samples in both parallel and perpendicular orientations relative to H_0.

To date, EPR measurements of muscle fibers have been

[1] To whom correspondence should be addressed. Fax: (518) 442-3462. E-mail: cps14@cnsvax.albany.edu.

1090-7807/00 $35.00

performed using modified metallized TE_{102} or TM_{110} cavities equipped with special sample ports and sample holders to accept a fiber-containing capillary in the parallel and in the perpendicular orientation[2] to the static magnetic field (*5–8*). However, weak intensity of EPR signals resulting from incomplete spin-labeling of the myosin heads (~40%) and overall low concentration of myosin heads in muscle (240 μM) have been the major progress-limiting factors in this field. Thus, an order-of-magnitude increase in overall system sensitivity is a worthwhile improvement for muscle spectroscopy.

It has recently been established that in many biophysical/biochemical EPR applications a substantial increase in sensitivity can be obtained while substituting metallic-wall cavities by miniature resonant structures containing dielectric resonators (DRs) (*11–15*). The advantages of these microwave EPR probe heads designed around low-loss high dielectric ceramics are their small size, high energy density at the sample position, good temperature stability, and low cost. In compact DRs, a high concentration of the magnetic component H_1 at the sample position leads to much higher filling factors (η) than in regular cylindrical or rectangular cavities. For instance, a double-stacked DR will have a 50-fold enhancement of η over a standard TE_{011} for the same sample capillary of 0.6 mm ID (*15*). Concomitantly, single- or double-stacked DR-based structures, resonating in the fundamental $TE_{01\delta}$ mode, have their electrical component E_1 mostly confined within high dielectric material, thus isolated from the sample space. The result is low dielectric loss and improved loaded resonator quality factor Q_L for aqueous sample capillaries positioned along the cylindrical axis of the DR. In combination with already-mentioned high filling factors, this leads to a high $Q_L \cdot \eta$ product, which improves the overall EPR sensitivity. It has also been found that the double-stacked DR-based structure could resonate in the fundamental $TE_{01\delta}$ mode, thus maintaining its intrinsic high Q_L and a steady separation from the first spurious mode, even when its total length (measured along the cylindrical axis) was elongated due to a finite spacing between the high dielectric cylinders (*14*). We explored these features to position a sample capillary in parallel to the external magnetic field through a horizontal guidance that was provided by an appropriately drilled hole in a low dielectric loss and low dielectric constant spacer inserted between the two DRs.

We present here the technical details and relevant performance of a compact double-stacked DR-based resonant structure that accepts longitudinal aqueous samples, such as muscle-fiber-containing capillaries, perpendicular and parallel to the external Zeeman field (H_0).

[2] Throughout this paper, the perpendicular orientation is an orientation of the sample tube which is perpendicular to the DC magnetic H_0 (Zeeman) field and parallel to the cylindrical axis of the DR, whereas the parallel orientation is an orientation of the sample tube which is parallel to the DC magnetic field and perpendicular to the cylindrical axis of the DR. The sample capillary is inserted through the side-access sample ports for the parallel orientation.

2. MATERIALS AND METHODS

Conventional EPR spectra (first harmonic, absorption in-phase) were acquired with the side-access DR-based resonant structure having the sample capillary in either parallel or perpendicular orientation to the magnetic field. The side-access DR was connected to the microwave bridge of a Bruker ER-200D spectrometer (Bruker Spectrospin, Billerica, MA) that was equipped with a low noise GaAsFET microwave amplifier before the crystal detector (Miteq, Model AMF-2S-8596-4). A standard TE_{102} cavity from Bruker, Model 4102 ST, was employed for acquiring reference spectra to those obtained in the side-access DR-based resonant structure. Throughout this work, thin-walled quartz capillaries from Vitro Dynamics (Rockaway, NJ) were used for holding test samples.

In its perpendicular orientation, the sample capillary was inserted through the vertical sample port and positioned along the cylindrical axis of the double-stacked DR. In this arrangement the sample capillary was aligned with the symmetry axis of the $TE_{01\delta}$ mode, thus probing the center space of the resonant structure where the magnetic component H_{1z} was the strongest. While loading the sample capillary in parallel to the external magnetic field we used the lateral sample ports. Since there was not enough space in the magnet gap, inserting the capillary in the parallel orientation had to be done with the resonator detached from the microwave bridge. The sample capillary that was oriented in the parallel orientation probed the space in between the ceramic resonators, thus intersecting the local minimum of H_{1z} for the fundamental $TE_{01\delta}$ mode.

For checking the EPR signal as a function of the microwave power in saturation measurements we employed an aqueous solution of 2,2,6,6-tetramethyl-4-piperidinol (from Aldrich) contained in a quartz capillary of 0.6-mm ID and 0.84-mm OD.

The local distribution of H_{1z} component along the parallel and perpendicular directions in the DR-based structure was checked using a point-DPPH (2,2-diphenyl-1-picrylhydrazyl from Sigma) sample whose linear dimension was less than 0.1 mm. The small speck of DPPH was held in the middle of a quartz capillary of 0.6-mm ID and 0.84-mm OD. The length of this capillary of ca. 60 mm was chosen to make it possible to easily change the point sample position while probing the whole active volume of the resonant structure. Therefore, the whole set of EPR spectra corresponding to different locations of the point sample along the parallel direction could be acquired without removing the DR-based resonator from the magnet gap.

The overall EPR performance of the side-access DR was checked using a 6.25 μM water solution of IASL, an iodoacetamide spin label (4-(2-iodoacetamido)-2,2,6,6-tetramethyl-1-piperidinyloxy from Aldrich) that was contained in a quartz capillary of 0.6-mm ID and 0.84-mm OD. We used the same sample capillary to acquire EPR spectra for the parallel and perpendicular sample orientations.

Bearing in mind the potential applications of the side-access DR-based structure, we also prepared small samples of spin-labeled muscle fibers. Single muscle fibers were isolated from rabbit psoas muscle. The fibers were ca. 5–6 mm long and their diameter ranged between 60 and 75 μm. A maleimide spin-label MSL (4-maleimido-2,2,6,6-tetramethyl-1-piperidinyloxy from Aldrich) exhibiting a high degree of order with respect to muscle fiber axis (*4*) was specifically attached to cys^{707} of the myosin head. Five doubled-up spin-labeled muscle fibers were transferred into a 0.6-mm-ID quartz capillary and infused with a glycerol-based buffer containing 130 mM KPr (potassium proprionate), 2 mM $MgCl_2$, 10 mM Mops, 1 mM EGTA, 50% glycerol (vol/vol). The presence of the buffer was necessary for keeping the muscle fibers intact during transportation and thaw-and-freezing cycles.

A baseline subtraction procedure was applied for the EPR spectra recorded in the side-access DR. Since the high dielectric ceramic for microwave applications is manufactured in a process of sintering of various metal oxides, some paramagnetic background signal is very often present in the spectra acquired in the DR. In particular, this baseline signal has to be taken into account when acquiring EPR spectra of weak paramagnetic systems.

EPR spectra of diluted (6.25 μM) aqueous solution of IASL spin label recorded in the side-access DR were baseline-corrected by subtracting the EPR spectrum of a capillary that was filled with distilled water. The baseline-correction procedure was also employed while acquiring broadened EPR features of spin-labeled muscle fibers.

A microwave test bench apparatus designed around the Hewlett Packard Sweep Oscillator, Model 8620C equipped with HP 86250D X-Band RF Plug-in was used for checking the Q_L-factor values for different loads and sample orientations in the DR-based structure. The same equipment was employed for checking the microwave response of a homebuilt TE_{011} cylindrical test cavity upon loading it with longitudinal aqueous samples in perpendicular and parallel directions. We used this cylindrical cavity as a reference for our double-stacked DR, since both devices reveal similar topology of the fundamental resonant modes. The TE_{011} cylindrical test cavity was equipped with lateral orifices and appropriate microwave cutoff elements to position the water-filled capillary oriented in a perpendicular orientation to its cylindrical axis. This sample orientation corresponded topologically to the parallel position in the DR-based structure.

3. TECHNICAL OUTLINE OF THE SIDE-ACCESS RESONATOR

The general scheme of the side-access EPR probe head is outlined in Fig. 1. The system was built around the double-stacked DR-based resonant structure described and modeled in Refs. (*14, 15*). We used two commercially available cylindrical DRs from MuRata-Erie (State College, PA) of the following dimensions: 6-mm OD, 2-mm ID, and 2.65-mm height. The DRs were separated from each other by a Rexolite (C-LEC Plastic, Inc., Beverly, NJ) spacer 1.8 mm thick. Rexolite is a cross-linked polystyrene that has excellent dielectric properties, i.e., low dissipation factor at microwave frequencies and low dielectric constant ($\epsilon_r = 2.53$ at 9.5 GHz). It has also good dimensional stability and is easily machined. In our previous experimental work we used cylindrical washers made of Rexolite to separate the two DRs in order to tune the structure to a desirable resonant frequency. For the present side-access probe head, the Rexolite separator was manufactured with holes that could accept and hold sample capillaries up to 1.0-mm OD in both parallel and perpendicular orientations. The hole drilled along the cylindrical axis of the washer accepted the sample capillary in an orientation perpendicular to the magnetic field, whereas the hole drilled diametrically accepted the sample capillary in an orientation parallel to the magnetic field.

The mechanical support for the ceramic resonators and for the spacer was provided by the Rexolite cylinder whose dimensions were 12.7-mm OD, 6.05-mm ID, and 14.0-mm height. Since the outer surface of this Rexolite element was metallized with a few micrometers of silver-plating, it also served as a microwave shield. The outermost shell of the resonant structure consisted of the Delrin cylinder equipped with lateral orifices that accommodated the antenna mount guide, as well as the guiding elements for the sample capillary oriented in parallel to the external magnetic field. The latter guiding elements, depicted as brass capillary adapters in Fig. 1, also served as microwave cutoff elements along this direction. Two flat cylindrical coils whose impedance was matched to a Bruker Model ER-022 signal channel provided the modulation field (H_M). These coils were firmly attached to the Delrin outer shell of the resonator body using two Nylon 1-72 screws. The Delrin-made cores of these coils had central orifices of 5 mm in diameter that accommodated the capillary guiding mounts. In order to avoid homogeneity distortions of the 100-kHz modulation field, we miniaturized the size of the brass capillary adapters so that their outer dimensions were 2.5-mm length, 2-mm OD, and 1.2-mm ID.

The 1.8-mm thickness of the Rexolite spacer between the DRs was such that the structure resonated at 9.54 GHz in its fundamental $TE_{01\delta}$ mode. The overall loaded quality factor, Q_L, of the empty resonant structure was 3400. The microwave power was routed to the resonant structure by a laterally positioned antenna. The plane of the coupling antenna was oriented perpendicular to the cylindrical axis of the resonant structure, thus coupling to the fundamental $TE_{01\delta}$ mode. The antenna and the adjacent impedance matching device were connected to the microwave bridge of the EPR spectrometer using a 12-in.-long section of 0.141-in. semirigid nonmagnetic coaxial cable and an appropriate coax-to-waveguide adapter.

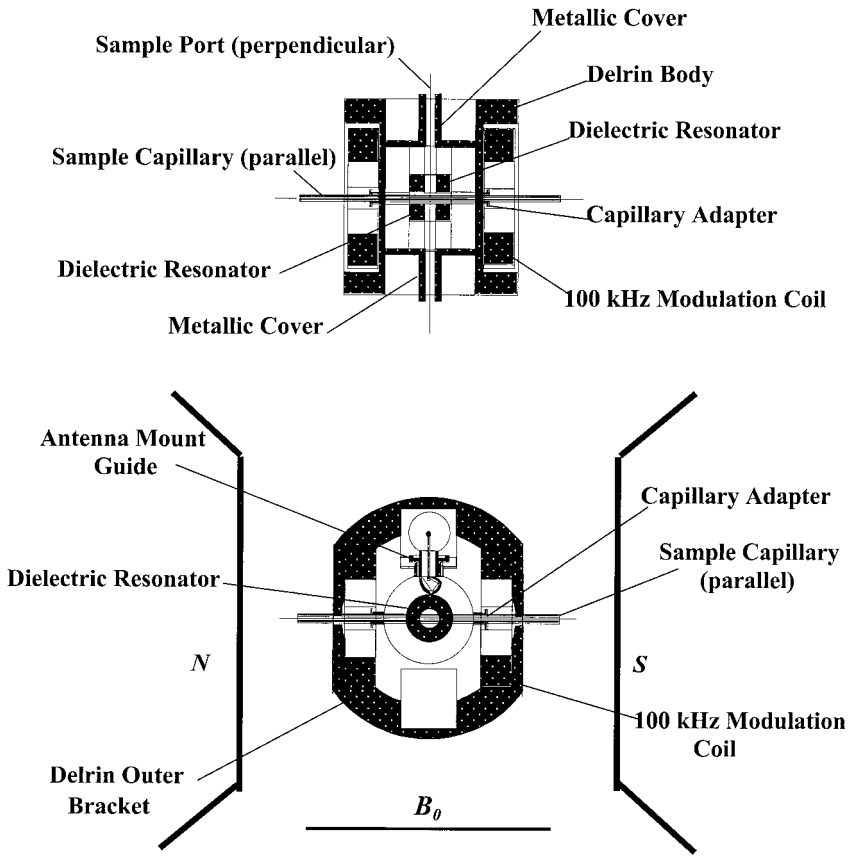

FIG. 1. Outline of the side-access double-stacked DR-based resonant structure: vertical cross-sectional (top) and horizontal cross-sectional (bottom) simplified drawings. The sample capillary is oriented parallel to the external magnetic field.

The external dimensions of the DR-based resonant structure shown in Fig. 1 were 27.3 mm (width) and 42 mm (height).

4. RESULTS AND DISCUSSION

4.1. Dielectric Loss in Aqueous Samples in the Double-Stacked DR

The dependence of the Q_L-factor of the double-stacked DR as a function of the inner diameter of water-filled quartz capillaries is shown in Fig. 2. The initial Q_L value for the empty resonant structure was ca. 3400 and gradually diminished upon loading with water-filled, thin-walled quartz capillaries (wall thickness in the range of 0.08–0.12 mm) of increasing inner diameter. The total sample length was ca. 50 mm, so that the entire active region of the probe head was used. For capillaries inserted through the side-access ports, i.e., oriented with sample perpendicular to the cylindrical axis of the structure (parallel orientation in the EPR experiment), the decrease in Q_L was less pronounced than for capillaries inserted along the cylindrical axis of the resonator (perpendicular orientation in the EPR experiment).

In the practical range of capillary inner diameters of 0.4 to 0.7 mm, the Q_L values for the parallel sample orientation were ca. 35% higher than for the perpendicular orientation. Theoretical estimates of the resonator Q_L-factor as a function of the capillary inner diameter are also shown in Fig. 2. These analytical curves calculated using a model developed in Ref. (*15*) also point to a lower dielectric loss and, consequently, higher Q_L values for sample capillaries oriented parallel to the magnetic field (perpendicular to the cylindrical axis of the double-stacked DR). Furthermore, the response of the double-stacked DR to loading with lossy capillary samples oriented either in parallel or perpendicular is distinctively different from that of a cylindrical TE_{011} cavity, even if the fundamental resonant modes of the DR and cavity bear similarity. Figures 3a and 3b and 4a and 4b show schematically the magnetic and electric field distribution patterns for the double-stacked DR-based structure and the standard TE_{011} cavity, respectively. These field patterns have been calculated using an analytical model reported in Ref. (*15*) for the double-stacked DR-based structure and standard expressions (*16*) for the TE_{011} cavity. The primary difference between the lowest resonant mode of cylindrical

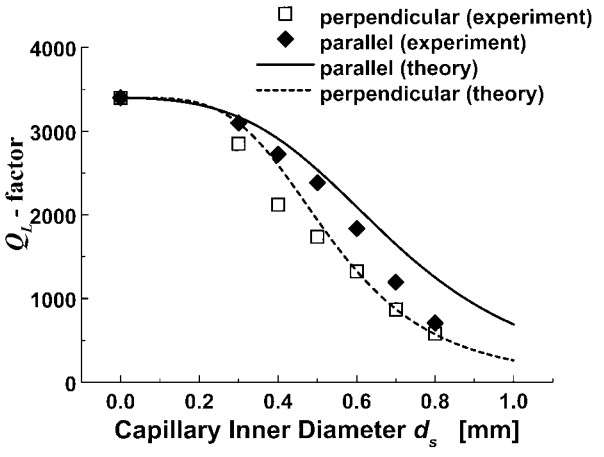

FIG. 2. Experimentally determined and theoretically estimated Q_L-factor changes in the double-stacked DR as a function of the capillary inner diameter (d_s) for quartz capillaries filled with distilled water. The open squares (□) and solid diamonds (◆) represent the experimental dependence of Q_L vs d_s for the perpendicular and parallel orientation of the sample capillary, respectively. The dashed line and solid line represent the theoretical estimate of Q_L vs d_s for the sample oriented in perpendicular and in parallel, respectively.

symmetry of the double-stacked DR ($TE_{01\delta}$) and TE_{011} cavity modes is their overall size. For the resonant frequency of ca. 9.4 GHz the typical dimensions are diameter of 12.7 mm and height of 14.0 mm for the $TE_{01\delta}$, wherease they are 42.0 mm and 44.9 mm for the TE_{011} cavity, respectively. However, as it is shown in Figs. 3a and 3b, the magnetic and electric field patterns for the double-stacked DR are also more complex. In contrast to the TE_{011} cavity mode, in the $TE_{01\delta}$ double-stacked DR mode there are two locations along the cylindrical axis where the magnetic component is the strongest, H_{1max} (Fig. 3a). Moreover, for the double-stacked DR the local minimum of electric component, E_{1min}, is located in the plane intersecting its structure at half height (Fig. 3b). This is also in striking contrast to the TE_{011} cavity mode, where the corresponding intersecting plane contains the locations of both H_{1max} and E_{1max}.

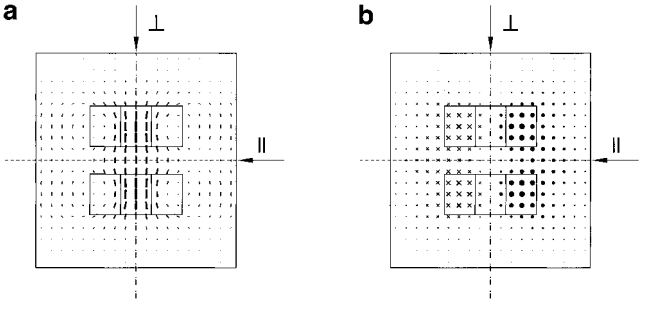

FIG. 3. Computed modal field distribution patterns for the $TE_{01\delta}$ mode of the double-stacked DR-based structure. (a) Distribution pattern of the magnetic component H_1. (b) Distribution pattern of the electric component E_1.

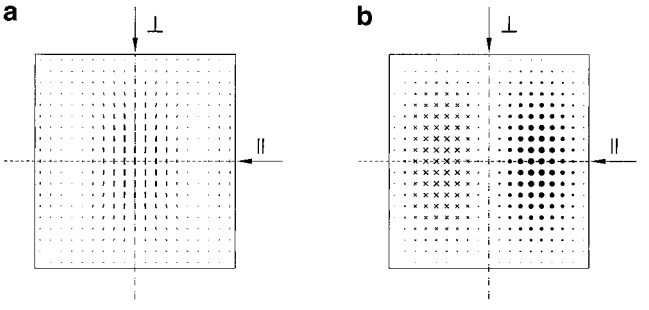

FIG. 4. Computed modal field distribution patterns for the cylindrical cavity TE_{011} mode. (a) Distribution pattern of the magnetic component H_1. (b) Distribution pattern of the electric component E_1.

The experimentally determined differences in microwave characteristics upon loading the double-stacked DR and the TE_{011} cavity with the same lossy aqueous sample are summarized in Table 1. As anticipated, based on the topology of the TE_{011} mode shown in Figs. 4a and 4b, loading the cavity in parallel with a 0.6-mm-ID capillary filled with water resulted in a much lower Q_L-factor value than that observed for the same capillary positioned in perpendicular. In contrast, for the double-stacked DR, the measured Q_L-factor for the parallel load was actually higher than that observed for the perpendicular capillary orientation. To explain these results, two aspects should be discussed in more detail.

First, the observed Q_L-factors for the parallel and perpendicular load with a lossy aqueous sample are of the same order of magnitude for both the TE_{011} cavity and the double-stacked DR. The similar Q_L values are obtained despite the fact that the aqueous sample oriented in parallel intersects the electric field lines, while the sample oriented in perpendicular mostly probes the nodal space of E_1. As it can be seen from Fig. 4b, the lossy longitudinal sample oriented in parallel in the TE_{011} cavity intersects the maximum of electric field, E_{1max}. This local maximum of the electrical component is located at the half height of the cavity cylinder, at the distance $r = 0.48\ (d/2)$ from the cylindrical symmetry axis, where d denotes the cavity diameter. A relatively low dielectric loss observed experimentally for a thin aqueous sample inserted in such an unfavorable

TABLE 1

Comparison of the Microwave Characteristics of the Double-Stacked DR-Based Structure Resonating in the $TE_{01\delta}$ Mode and of the TE_{011} Cylindrical Cavity upon Loading with a 0.6-mm-ID Capillary Filled with Distilled Water for Parallel and Perpendicular Sample Positions

	Q_L empty	$Q_{L\parallel}$	$Q_{L\perp}$	$\Delta f_{0\parallel}$ (MHz)	$\Delta f_{0\perp}$ (MHz)
DR ($TE_{01\delta}$)	3400	1840	1330	−10	−2.7
Cavity (TE_{011})	6400	3180	4800	−74	−10

way can be explained by realizing that for the parallel sample orientation the electric field lines are perpendicular to the sample capillary. Therefore, a thin water-filled capillary can be regarded as a longitudinal object having high dielectric constant and high dielectric loss at X-band microwave frequencies. Simple analysis of a dielectric rod immersed in the locally homogeneous electric field perpendicular to its axis shows that, in the quasi-static approximation, the E_1 field amplitude within the dielectric is reduced by a factor of $(\epsilon + 1)/2$ (*17*), where ϵ denotes the complex permittivity of the dielectric. Taking a typical value of $\epsilon = 62 - i30$ for water at 9.3 GHz (*18*) and neglecting the influence of a thin-walled capillary, one can find dielectric losses to be ca. 3 orders of magnitude lower than those expected from a direct application of the perturbation formula (*19*). In practice, however, the above analysis for a capillary oriented in parallel can be regarded as a rough approximation only, mainly because the electric field E_1 is not entirely homogeneous within the sample region. In particular, for both the TE_{011} (cavity) and the $TE_{01\delta}$ (DR) modes, lines of the electric component form closed circles in the plane that intersects the sample capillary. Curvature of the E_1 lines results in a small contribution of the electric component that is parallel to the capillary axis. It can be shown that this small contribution is responsible for the major part of dielectric losses, whereas the electric field component perpendicular to the sample axis is effectively screened. As a result, the Q_L-factor for the parallel orientation is of the same order of magnitude as for the standard (perpendicular) sample orientation for both the TE_{011} cavity and the double-stacked DR-based resonant structure.

Second, to interpret the experimental results for the double-stacked DR loaded with a lossy sample oriented in parallel we should compare the topology of its resonant mode to the well-known TE_{011} cavity mode. As it has been mentioned, in the TE_{011} cavity the capillary oriented in parallel intersects the electric field in its maximum, whereas in the double-stacked DR structure the sample probes a much weaker E_1 field in the space between dielectric resonators. As seen from Fig. 3b, for the axially symmetric double-stacked DR resonating in the $TE_{01\delta}$ mode the electric component is mainly confined to the high dielectric cylinders. As a result, in the double-stacked DR the dielectric losses for the parallel orientation are diminished, thus yielding $Q_{L\parallel} > Q_{L\perp}$. In contrast, in the TE_{011} cavity the Q_L-factor for the parallel capillary orientation ($Q_{L\parallel}$) is lower than for the standard perpendicular orientation ($Q_{L\perp}$). It is also worth noting that the resonant frequency shift upon loading the water-filled 0.6-mm-ID capillary in parallel ($\Delta f_{0\parallel}$) was more pronounced for the cavity than for the DR. Similarly, for the perpendicular sample orientation, the corresponding resonant frequency shift ($\Delta f_{0\perp}$) was also more marked for the TE_{011} cavity than for the DR. This may account for better isolation of E_1 from the sample space in the dielectric resonator in either of the capillary orientations. The frequency shifts, measured with respect to the resonant frequency of the empty cavity or empty double-stacked DR resonator, are listed in Table 1.

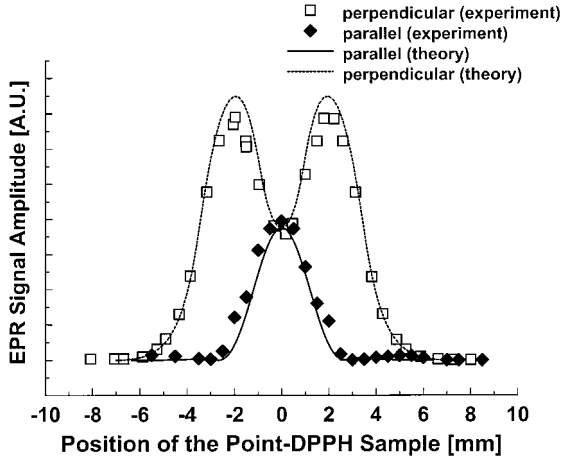

FIG. 5. Theoretical estimate and experimentally measured variation of the magnetic component H_{1z}^2 in the side-access double-stacked DR. A point-DPPH sample was used for probing the local EPR signal intensity (proportional to H_{1z}^2) along the perpendicular and parallel directions. The dashed and solid lines depict the theoretically estimated H_{1z}^2 distributions along the perpendicular and parallel directions, respectively. The open squares (□) represent the experimentally measured H_{1z}^2 distribution along the perpendicular direction. The solid diamonds (◆) represent the experimentally measured H_{1z}^2 distribution along the parallel direction. Experimental conditions: gain = 2000, modulation = 0.125 G, time constant t_c = 0.1 ms, sweep 20 G/50 s, microwave power = 2 mW.

4.2. H_{1z}^2 Distribution in the Double-Stacked DR for the Parallel and Perpendicular Capillary Orientations

For constant incident power, the variation in EPR signal intensity with sample position in the resonant structure depends upon H_{1z}^2 (*15, 20*). Figure 5 compares the results of the experimentally measured and theoretically estimated distributions of H_{1z}^2 for perpendicular and parallel sample orientation in the double-stacked DR. The experimental points correspond to the amplitude of the EPR signal ($d\chi''/dH$) yielded by a point-DPPH sample that was moved along both probing directions in the DR. All of the EPR spectra were acquired at a constant and nonsaturating incident microwave power of 2 mW. Since the resonator Q_L-factor was independent of the point-DPPH sample position in either of the probing directions, the local minimum of H_{1z}^2 for the perpendicular direction overlapped with the local maximum of H_{1z}^2 for the parallel direction. For this characteristic value of H_{1z}^2 the point-DPPH sample was located in the geometrical center of the double-stacked DR. The analytical fits shown in Fig. 5 (solid line for the parallel orientation and dashed line for the perpendicular orientation) were calculated using the theoretical model described in Ref. (*15*) and are in a qualitatively good agreement with the experimental results. For the sample capillary oriented perpendicular to the

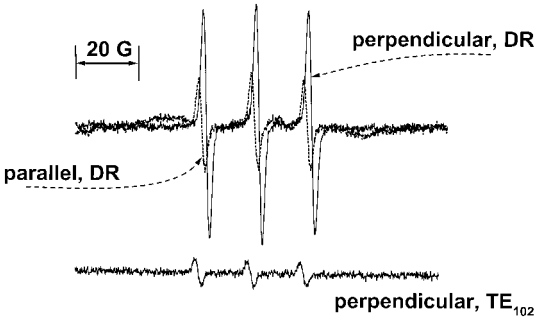

FIG. 6. EPR spectra recorded for a 6.25 μM aqueous solution of IASL spin-label. The EPR traces acquired in the double-stacked DR for perpendicular and parallel capillary orientations were background-corrected. Normalized experimental conditions for the experiments using the side-access DR and TE_{102} cavity: gain = 10^5, modulation = 1.6 G, time constant = 50 ms, sweep 120 G/100 s, microwave power = 2 mW.

external magnetic field, the apparent discrepancy between the theoretical and experimental H_{1z}^2 distributions (up to ca. 10% around local maximum values) is mainly due to a strong perturbation of the $TE_{01\delta}$ mode by the presence of the 2-mm center hole in the high dielectric ceramic cylinders.

4.3. Sensitivity Tests for a Lossy Sample Oriented Parallel and Perpendicular to the External Magnetic Field

Results of the sensitivity tests for a lossy sample oriented either in parallel (side-access) or in perpendicular (vertical access) with respect to the Zeeman field are shown in Fig. 6. The EPR spectra were obtained for a 6.25 μM aqueous solution of IASL spin-label that was contained in the quartz capillary of 0.6-mm ID and 0.84-mm OD. For the perpendicular sample orientation, the observed signal amplitude was ca. 2.5 times bigger than for the parallel (side-access) position. Lower signal amplitude for the parallel orientation was in fact anticipated taking into account the theoretical estimates of H_{1z}^2 and experimental mapping with the point-DPPH sample. Integrals of the experimentally determined H_{1z}^2 distribution curves shown in Fig. 5 correspond to filling factors that one might expect for a long nonlossy sample oriented either in parallel (filling factor $\eta_{\|}$) or in perpendicular (filling factor $\eta_{\perp}$) with respect to Zeeman field. The ratio of these surfaces, which is proportional to $\eta_{\|}/\eta_{\perp}$, was found to be 0.28. On the other hand, the Q_L-factor ratio for a lossy longitudinal sample, $Q_{L\|}/Q_{L\perp}$, was found to be 1.38 (values of $Q_{L\|}$ and $Q_{L\perp}$ are listed in Table 1). The product of these two expressions yielded a factor of 0.39 that should represent to the overall sensitivity loss for the parallel orientation of the sample capillary. This estimate is in good agreement with the EPR signal amplitude ratio of 0.40 observed experimentally for the sample capillary oriented either in parallel or perpendicular with respect to the external magnetic field.

For comparison of the performances, in Fig. 6 we also show the EPR spectrum recorded for the same 6.25 μM IASL sample in the TE_{102} cavity. This spectrum was acquired in the perpendicular sample orientation, since our standard TE_{102} cavity did not provide side-access for the sample capillary. For the perpendicular sample orientation, the spectra recorded in the DR-based structure revealed ca. 10 times higher signal-to-noise ratio than for the TE_{102} cavity. Although the spectra acquired in the DR were baseline-corrected, the final EPR traces presented in Fig. 6 reveal some presence of the paramagnetic background. This incomplete baseline subtraction was more marked for the parallel capillary orientation and was caused by different dielectric properties of aqueous liquids in the test IASL sample and in the water-filled capillary that was used for acquiring the background signal. Small misalignments of the sample capillary in the parallel sample orientation can also result in slightly different perturbations of the $TE_{01\delta}$ mode of the double-stacked DR. Since the surface of the high dielectric ceramics has anisotropic paramagnetic properties, differences in probing of this local paramagnetic background can also account for an incomplete baseline subtraction.

4.4. EPR Results for Spin-Labeled Muscle Fibers

The EPR results obtained in the side-access DR-based resonant structure for specifically spin-labeled muscle fibers are shown in Fig. 7. As expected, two distinctively different spectra were obtained for parallel (side-access) and perpendicular orientation (regular access) of the fiber-containing capillary with respect to the Zeeman field. When the fiber bundle was placed parallel to the magnetic field, a characteristic spectrum consisting of three lines with narrow splitting of 17.5 G between the outer extrema was observed. The hyperfine features

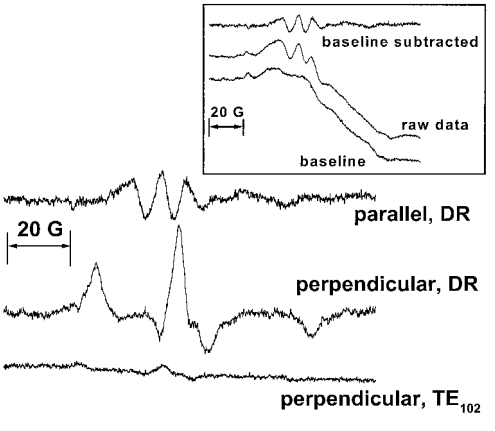

FIG. 7. EPR spectra acquired for a small bundle of muscle fibers specifically spin labeled at cys^{707} of myosin head. Fibers were immersed in glycerol and held in a 0.6-mm-ID, 0.84-mm-OD quartz capillary. Inset: EPR traces for the baseline subtraction acquired for the muscle fiber sample oriented in parallel in the double-stacked DR. Normalized experimental conditions: gain = 10^5, modulation = 1.6 G, time constant = 50 ms, microwave power = 2 mW, sweep 120 G/100 s; 10 scans were acquired for each trace.

observed in this EPR spectrum reveal a considerable broadening that is typical for a highly oriented population of strongly immobilized spin probes when there is little or no motion of the probe on the microsecond time scale. For such a parallel orientation of the muscle fiber, the principal *z*-axis of the MSL spin label is approximately perpendicular to the magnetic field, while being also approximately perpendicular (82°) to the fiber axis. [According to Ref. (*4*), the tilt angle of the principal *z*-axis of a nitroxide spin label with respect to the fiber axis (i.e., the axis having maximum hyperfine coupling) is 82° with a Gaussian RMS distribution in angular disorder of ±7°.]

In contrast, a broad quasi-powder pattern was obtained when the fiber-containing capillary was placed in perpendicular orientation to the magnetic field. Such an EPR spectrum with wide peak-to-peak splitting between the outer extrema of 70.2 G is to be expected when the principal *z*-axes of the MSL spin labels are aligned mostly parallel to the external magnetic field, being also perpendicular to the fiber axis. In Fig. 7 we also show the EPR spectrum obtained for the same sample in the TE_{102} cavity (perpendicular orientation). For the muscle bundle inserted in perpendicular orientation to the Zeeman field, the DR-based structure yielded ca. 10 times better S/N ratio than the standard TE_{102} cavity. When the same muscle fiber was in the parallel orientation in the DR, the S/N was roughly 2.5 times lower. In similarity to the difference in the S/N observed for aqueous solutions between parallel and perpendicular orientations, the lower S/N observed for the parallel orientation of the muscle fiber is due to the poorer filling factor $\eta_{\|}$. The inset to Fig. 7 shows the paramagnetic background of the double-stacked DR used for these preliminary test measurements of muscle fibers. The EPR traces shown in this inset were acquired for the sample capillary oriented in parallel to the Zeeman field. It is worthwhile to mention that due to the topology of the $TE_{01\delta}$ double-stacked DR, the paramagnetic background for the sample oriented in perpendicular was slightly different from that in parallel. Accordingly, a corresponding trace of the baseline was taken into account in order to generate the EPR spectrum of the muscle fiber oriented in perpendicular in the double-stacked DR.

5. CONCLUSIONS

We built and successfully tested the specialized probe head for the EPR study of muscle fibers. The microwave heart of this probe is based on the double-stacked DR-based resonant structure. Due to the finite separation of 1.8 mm between the cylindrical DRs, this EPR probe readily accepts capillaries containing aqueous samples oriented parallel with respect to the Zeeman field (i.e., normal to the cylindrical axis of the resonant structure). The topology of the $TE_{01\delta}$ mode in such a double-stacked DR imposes smaller filling factors for the parallel sample orientation than for the more commonly used perpendicular orientation. Nonetheless, both microwave test bench results and theoretical calculations point to lower dielectric loss for aqueous samples oriented parallel to the magnetic field. The observed and estimated Q_L-factors are then higher for the parallel sample orientation, thus partially compensating for the lower filling factor $\eta_{\|}$. As a result, for the parallel orientation the observed sensitivity is only ~2.5 times worse than for the perpendicular sample orientation that is generally employed in typical applications of the DR-based structures.

For lossy aqueous solutions and for small bundles of muscle fibers, the double-stacked DR revealed a higher signal-to-noise than the standard TE_{102} cavity. For a diluted (6.25 μM) aqueous solution of the IASL spin label contained in the sample capillary in the perpendicular orientation, the tested DR-based structure yielded a ca. 10 times larger S/N ratio than a standard TE_{102} cavity. With the capillary inserted parallel to the external magnetic field, in spite of the lower filling factor for this direction ($\eta_{\|}$), the S/N ratio yielded by the side-access DR was still ~4 times better than in the TE_{102} cavity with the sample placed in perpendicular orientation.

EPR results obtained for small bundles of muscle fibers also indicate that the DR-based device loaded either in perpendicular (regular access) or in parallel (side-access) outperforms the regular TE_{102} cavity. For such small muscle fiber samples oriented in perpendicular in the DR, the S/N was found to be at least 10 times better than for the TE_{102} cavity. For the parallel orientation in the double-stacked DR, due to the lower filling factor, the signal-to-noise ratio was lower, still *ca.* 4 times better than for the TE_{102} cavity.

ACKNOWLEDGMENTS

The authors particularly acknowledge Dr. Huichun Li, NHMFL (Tallahassee, FL), for her technical help with preparation of the muscle fibers. We are also grateful to Mr. R. A. Isaacson, Department of Physics, UCSD, for many stimulating discussions regarding the DR-based technology. This work has been supported by the U.S.–Poland Maria Sklodowska-Curie Joint Fund II, PAN/NIST-94-203, by Polish KBN Grant 2-PO3B-018-13 (A.S.), and by the NSF IBN-98-08708 and IHRP-NHMFL grants (P.F.). A.S. also acknowledges the State of Florida supported NHMFL Visitors Program, Project 1431. Acknowledgement is made to the donors of the Petroleum Research Fund, administered by the American Chemical Society, for partial support of this research (through ACS-PRF Grant 34132 AC4 to C.P.S.).

REFERENCES

1. A. F. Huxley, *Science* **164,** 1355 (1969).
2. A. F. Huxley and R. M. Simmons, *Nature* **233,** 533 (1971).
3. J. A. Spudich, *Nature* **372,** 515 (1994).
4. D. D. Thomas, *Annu. Rev. Physiol.* **49,** 691 (1987).
5. O. Roopnarine and D. D. Thomas, *Biophys. J.* **67,** 1634 (1994).
6. P. G. Fajer, R. L. H. Bennett, C. F. Polnaszek, E. A. Fajer, and D. D. Thomas, *J. Magn. Reson.* **88,** 111 (1990).
7. D. D. Thomas, S. Ishiwata, J. C. Seidel, and J. Gergely, *Biophys. J.* **32,** 873 (1980).
8. D. D. Thomas and R. Cooke, *Biophys. J.* **32,** 891 (1980).

9. P. G. Fajer, *Proc. Natl. Acad. Sci. USA* **91,** 937 (1994); P. G. Fajer, *Biophys. J.* **66,** 2039 (1994).

10. J. W. Orton, "Electron Paramagnetic Resonance," pp. 75–78, Iliffe, London (1968).

11. R. W. Dykstra and G. D. Markham, *J. Magn. Reson.* **69,** 350 (1986).

12. K. Qu, J. Vaughn, A. Sienkiewicz, C. P. Scholes, and J. S. Fetrow, *Biochemistry* **36,** 2884 (1997).

13. A. Sienkiewicz, A. M. da Costa Ferreira, B. Danner, and C. P. Scholes, *J. Magn. Reson.* **136,** 137 (1999).

14. A. Sienkiewicz, K. Qu, and C. P. Scholes, *Rev. Sci. Instrum.* **65**(1), 68 (1994).

15. M. Jaworski, A. Sienkiewicz, and C. P. Scholes, *J. Magn. Reson.* **124,** 87 (1997).

16. C. P. Poole, "Electron Spin Resonance: A Comprehensive Treatise on Experimental Techniques," pp. 270–272. Wiley–Interscience, New York (1967).

17. J. A. Stratton, "Electromagnetic Theory," McGraw-Hill, New York (1941).

18. J. P. Barnes and J. H. Freed, *Rev. Sci. Instrum.* **68**(7), 2838 (1997).

19. R. F. Harrington, "Time-Harmonic Electromagnetic Fields," McGraw-Hill, New York (1961).

20. M. Sueki, G. A. Rinard, S. S. Eaton, and G. R. Eaton, *J. Magn. Reson. A* **118,** 173 (1996).